# Three-Dimensional Structure of Rat Surfactant Protein A Trimers in Association with Phospholipid Monolayers[†,‡]

Nades Palaniyar,*[,§,||] Francis X. McCormack,[§] Fred Possmayer,[⊥] and George Harauz[||]

*Division of Pulmonary/Critical Care Medicine, Department of Internal Medicine, University of Cincinnati, 231 Bethesda Avenue, Cincinnati, Ohio 45267-0564, Department of Molecular Biology and Genetics, University of Guelph, Guelph, Ontario, Canada N1G 2W1, and Medical Research Council Group in Fetal and Neonatal Health and Development, Departments of Obstetrics and Gynecology and Biochemistry, University of Western Ontario, London, Ontario, Canada N6A 5A5*

*Received December 6, 1999; Revised Manuscript Received March 8, 2000*

ABSTRACT: Surfactant protein A (SP-A) is a C-type lectin found primarily in the lung and plays a role in innate immunity and the maintenance of surfactant integrity. To determine the three-dimensional (3D) structure of SP-A in association with a lipid ligand, we have used single particle electron crystallography and computational 3D reconstruction in combination with molecular modeling. Recombinant rat SP-A, containing a deletion of the collagen-like domain, was incubated with dipalmitoylphosphatidylcholine: egg phosphatidylcholine (1:1, wt/wt) lipid monolayers in the presence of calcium, negatively stained, and examined by transmission electron microscopy. Images of SP-A−lipid complexes with different angular orientations were used to reconstruct the 3D structure of the protein. These results showed that SP-A subunits readily formed trimers and interacted with lipid monolayers exclusively via the globular domains. A homology-based molecular model of SP-A was generated and fitted into the electron density map of the protein. The plane of the putative lipid−protein interface was relatively flat and perpendicular to the hydrophobic neck region, and the cleft region in the middle of the trimer had no apparent charge clusters. Amino acid residues that are known to affect lipid interactions, $Glu^{195}$ and $Arg^{197}$, were located at the protein−lipid interface. The molecular model indicated that the hydrophobic neck region of the SP-A did not interact with lipid monolayers but was instead involved in intratrimeric subunit interactions. The glycosylation site of SP-A was located at the side of each subunit, suggesting that the covalently linked carbohydrate moiety probably occupies the spaces between the adjacent globular domains, a location that would not sterically interfere with ligand binding.

Surfactant protein A (SP-A)[1] is the most abundant protein associated with pulmonary surfactant (*1*). SP-A is found in association with surfactant lipids in a variety of intracellular and extracellular environments, including lipid vesicles and lamellar bodies, and specialized membranes such as tubular myelin. In addition, SP-A has been reported to associate with the surface of a number of microorganisms and pollen grains and to exist as free molecules in aqueous environments (*2*, *3*). The existence of such diverse ligands for SP-A, and SP-A's abundance in the alveolar environment, suggest that it may be involved in multiple functions. In vitro studies have implicated SP-A in regulation of lipid secretion from type II cells, formation of tubular myelin, adsorption of lipids to the air−water interface, lipid recycling, lipid vesicle aggregation, prevention of serum protein-induced inhibition of the surface active properties of surfactant, opsonization of microorganisms, induction of chemotaxis, and microbial killing by phagocytes (*2*−*5*). Recent transgenic mouse studies support roles for SP-A in the formation of tubular myelin (*6*), in preventing serum protein-induced inhibition of surfactant function (*7*, *8*), and in innate immune function in vivo (*9*, *10*). The absence or over-abundance of SP-A in mice does not affect the surfactant pool sizes (*8*, *11*), suggesting that either SP-A is not involved in surfactant homeostasis or that other redundant pathways exist that control surfactant secretion and uptake. Another structurally related surfactant protein, SP-D, may be involved in such functions (*12*−*14*).

The primary structures of SP-A from several organisms are highly homologous, and mutagenesis studies of rat SP-A reveal the existence of several distinct functional domains (*5*, *15*, *16*). The rat SP-A molecule is composed of a short

[†] This work was supported by the research grants of the Ontario Thoracic Society (G.H.), MRC Group Grant M268C7 (F.P.), Career Investigator Award from American Lung Association (F.X.M.), Veterans' Affairs Merit Award (F.X.M.), and NIH HL61612 (F.X.M). N.P. is a recipient of an American Lung Association and a Canadian Lung Association/Canadian Medical Research Council Postdoctoral Fellowship.

[‡] Protein Data Bank Accession No. 1DU8; Research Collaboratory for Structural Bioinformatics Accession No. RCSB010373.

* Corresponding author: Division of Pulmonary/Critical Care Medicine, Department of Internal Medicine, University of Cincinnati, 231 Bethesda Ave, Cincinnati, OH 45267-0564. Telephone: (513)558-4831 or 558-3859; Fax: (513)558-4858; E-mail: nadesap@ucmail.uc.edu.

[§] University of Cincinnati.

[||] University of Guelph.

[⊥] University of Western Ontario.

[1] Abbreviations: CRD, carbohydrate recognition domain; DPPC, dipalmitoylphosphatidylcholine; egg PC, unsaturated phosphatidylcholine from egg; MALDI-MS, matrix-assisted laser desorption ionization mass spectrometry; MBL, mannose binding lectin; SP-A, surfactant protein A; TEM, transmission electron microscopy.

10.1021/bi992793b CCC: $19.00 
Published on Web 05/04/2000

N-terminal region, a collagen-like domain with Gly−X−Y repeats, a hydrophobic neck region, and a C-terminal globular carbohydrate recognition domain (CRD). Low-resolution structures of SP-A from different species have been elucidated by a variety of techniques (*17*−*19*) including transmission electron microscopy (TEM) (*20*−*23*). These studies show that six triple helices interact to form a common stem with a bouquet of flower-like quaternary structure. Recently, Palaniyar et al. (*22*) have demonstrated the existence of a supraquaternary structure for bovine SP-A and described its interaction with the surfaces of lipid monolayers and bilayers (*22*, *24*, *25*) using TEM. These studies (*21*, *22*) were consistent with prior studies that suggested that the C-terminal globular domain of SP-A interacted with lipid surfaces in a calcium-dependent manner (*5*).

High-resolution structural information on SP-A is not available. Furthermore, the mechanism by which SP-A interacts with its lipid ligands is also not clearly understood. Here we describe the three-dimensional (3D) structure of a truncated form of recombinant SP-A interacting with a lipid ligand determined by a combination of electron microscopy and molecular modeling.

## EXPERIMENTAL PROCEDURES

*Protein Purification.* Recombinant baculovirus expressing a cDNA for the collagen-like domain deleted form of rat SP-A (SP-A$^{\Delta G8-P80}$) (*26*) was used to infect freshly plated *Trichoplusia ni* insect cells at a multiplicity of infection of 10. Infected cells were grown for 72 h in serum-free Ex-Cell 400 media (J. R. H. Biosciences, Lenexa, KS). Proteins in the cell-free media were adsorbed to a mannose-Sepharose 6B column in the presence of 10 mM $CaCl_2$, and the recombinant SP-A was eluted from the column with 2 mM EDTA. Purified protein was stored at −20 °C after dialysis against 5 mM Tris-HCl (pH 7.4).

*Determination of Glycosylation State of CRD.* Matrix-assisted laser desorption ionization mass spectrometry (MALDI-MS) was used to determine the approximate mass of the carbohydrate modifying Asn$^{187}$ of the CRD.

*Preparation of Specimen and Electron Microscopy.* Recombinant SP-A (13 $\mu$L of 20−100 $\mu$g/mL) was placed in a 3 (diameter) × 1 mm (depth) Teflon well in the presence of 50 $\mu$M−1 mM $CaCl_2$. To generate lipid monolayers, a volume of 0.7−1 $\mu$L of dipalmitoylphosphatidylcholine (DPPC):egg phosphatidylcholine (egg PC) mixture (1:1, wt/wt, 0.4 mg/mL) dissolved in chloroform:hexane (1:1, vol/vol) (Avanti Polar Lipids, AL) was touched to the air−liquid interface and incubated at 37 °C for 1−2 h. A holey plastic-containing copper grid (200 or 400 mesh) that was stabilized by a thin layer of evaporated carbon was touched onto the lipid monolayer surface. The specimen grid was then placed on a drop of saturated solution of uranyl acetate (2−4%) for 30−60 s, and the excess stain was removed with torn filter paper. The stained grid was air-dried for at least 1 h before examination with TEM. Specimens were examined and photographed using a JEOL JEM-100CX or 100CX-II TEM at 66 000× nominal magnification.

*3D Reconstruction.* Negatives were digitized using a CCD camera and Winview software (Princeton Instruments, EMPIX, Mississauga, ONT, Canada) at 2.0 Å object/picture element (pixel). Over 3000 negatively stained particles were interactively selected, and density information was extracted from an 80 × 80 pixels area around visually selected center points using IMAGIC-V (*27*, *28*). This population of images (2D electron density profiles) was computationally aligned, sorted, and classified by multivariate statistical techniques (*29*). After three cycles of this process, a converged population of 60 two-dimensional "class averages", with each class representing a relatively homogeneous subgroup of images of individual complexes, was obtained. These images represented views of the SP-A$^{\Delta G8-P80}$ complex in different orientations with greater clarity than individual images. To calculate the average dimension of SP-A$^{\Delta G8-P80}$, distance between opposite edges of the electron dense regions (2−3 measurements for each 2D class average) was measured. The relative 3D orientations of the SP-A$^{\Delta G8-P80}$ complexes in these averages were obtained by an iterative quaternion-assisted angular determination process (*27*−*29*), and 3D reconstruction was thereby completed. This 3D electron density map was displayed using INSIGHT II/97 molecular modeling software (MSI, San Diego, CA) and used to define the contour of the complex for fitting of the molecular model.

*Molecular Modeling.* A homology-based molecular model of SP-A$^{\Delta G8-P80}$ was generated using the appropriate regions of the amino acid sequence of rat SP-A (*16*) and the X-ray crystallographic coordinates of the corresponding neck/CRD regions of the homologous protein, mannose binding lectin (MBL) (*30*). Modeling was done using INSIGHT II/97 software on an IBM RISC/6000 Powerstation 3AT. Briefly, to generate the molecular model, the X-ray crystallographic coordinates of MBL (1hup) were downloaded from the Brookhaven Protein Data Bank, and the sequence was extracted. Coordinates of highly homologous regions in the CRD domains of MBL were used to assign the coordinates for corresponding regions of SP-A. Two remaining segments of the SP-A CRD, Thr$^{135}$−Arg$^{146}$ and Lys$^{201}$−Lys$^{203}$, did not show significant homology with MBL and were generated as loops. Three criteria were used for finding the most appropriate loop: (a) smaller root-mean-square value, (b) overall structural similarity to the corresponding region of the MBL molecule, and (c) absence of steric hindrance. Although the sequence homology in the neck regions of these two proteins was limited, a similar structure could still be predicted. Hence, the amino acid sequence of the SP-A neck region was assigned to the structural coordinates of the MBL neck region. Since the cysteines of the CRD that are involved in disulfide bridge formation were conserved, these residues were linked in the model in the same pattern as is found for MBL and all other C-type lectins that have been characterized (*3*, *5*, *31*). In the absence of any X-ray crystallographic data, and on the basis of the secondary structure prediction, the seven amino acids of the N-terminal segment of SP-A were assigned a random coil configuration. Ends of this molecule were defined, and the splice junctions were repaired. Finally, the molecular model was subjected to adjustment of parameters by energy minimization.

*Fitting the Molecular Model to the SP-A Electron Density Profile.* The SP-A$^{\Delta G8-P80}$ molecular models were organized as trimers such that the neck region of the protein was assembled through hydrophobic interactions similar to those found in other lectins (*30*, *32*, *33*). These trimers

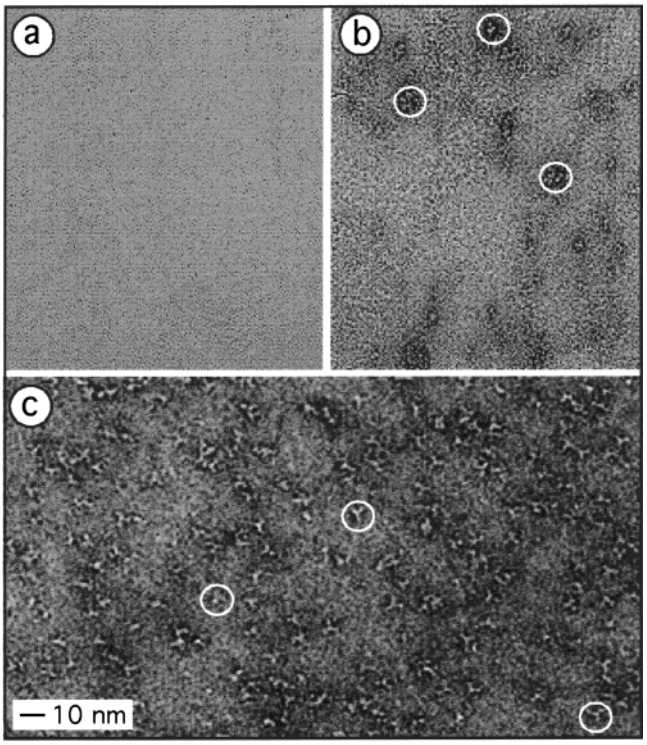


FIGURE 1: TEM images of collagen-like domain deleted recombinant SP-A in association with lipid monolayers. Recombinant SP-$A^{\Delta G8-P80}$ was incubated with DPPC:eggPC monolayers (1:1, wt/wt) at 37 °C for 2 h and negatively stained with uranyl acetate. DPPC:eggPC monolayers are shown (a) without SP-A and with 50 $\mu$M $CaCl_2$, (b) with SP-A and 1 mM EDTA, and (c) with SP-A and 50 $\mu$M $CaCl_2$.

were interactively placed into the 3D electron density map of the protein using INSIGHT II/97. Various threshold levels were further applied to eliminate the background noise from the 3D electron density map.

## RESULTS

*Recombinant Rat SP-A Forms Trimers.* To obtain images of isolated single particles of SP-A, the recombinant protein was allowed to interact with lipid monolayers. The protein−lipid film was picked up by a grid, negatively stained, and imaged by TEM. The DPPC:egg PC (1:1, wt/wt) monolayers were smooth and free of any negatively stained particles in the absence of SP-A (Figure 1a). When SP-A interacted with the monolayers in the presence of a chelating agent, 1 mM EDTA, only a limited number of SP-A trimers interacted with the ligand (Figure 1b). However, in the presence of 50 $\mu$M $CaCl_2$, SP-A trimers were readily detected (Figure 1c). These molecules were visually identifiable as trimers by their characteristic "trillium" shape (Figure 1c, circle) and were approximately 7 nm in size. The trimeric organization and dimensions were similar even when this protein was spread on carbon film, negatively stained, and viewed by TEM (data not shown). The molecular weight of the SP-$A^{\Delta G8-P80}$, determined by darkfield scanning TEM methods (*34*), was also consistent with a trimeric stoichometry (Palaniyar et al., unpublished data). These results showed that the SP-$A^{\Delta G8-P80}$ readily formed calcium-independent trimers but interacted with lipid monolayers in a calcium-dependent manner. Furthermore, SP-$A^{\Delta G8-P80}$ trimers were evenly distributed on the DPPC:eggPC (1:1, wt/wt) monolayer surface at 50 $\mu$M $CaCl_2$ concentration with minimal protein−protein interaction.

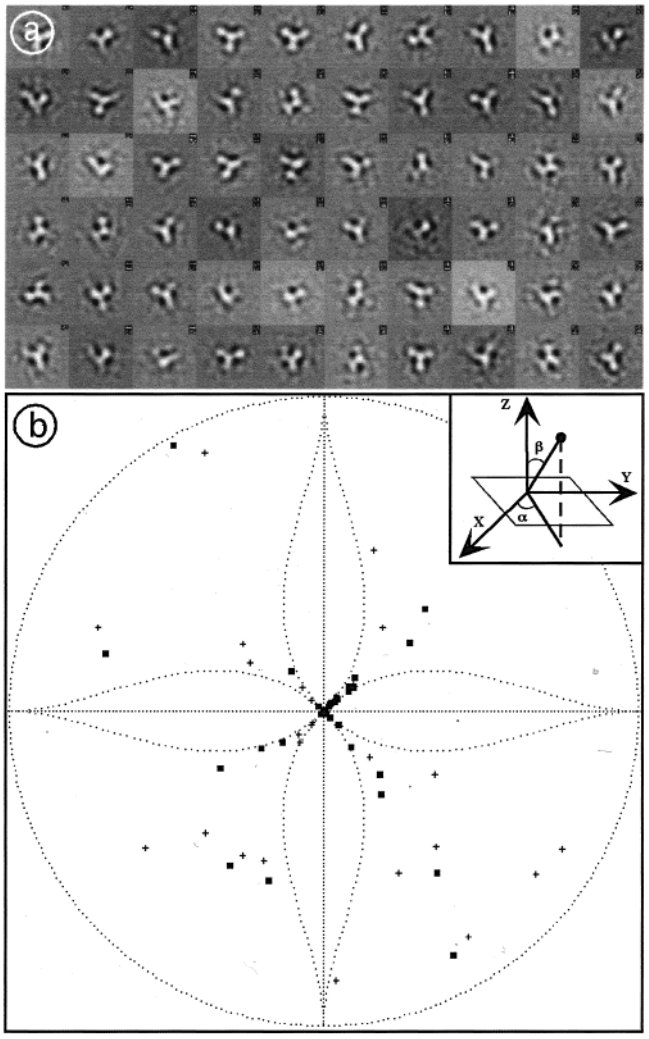


FIGURE 2: 2D averages of SP-$A^{\Delta G8-P80}$ trimers. (a) Images of 3035 isolated trimers were mathematically classified into 60 homogeneous subgroups using IMAGIC-V. Note the trillium-like configuration of the trimers. Average dimension of the trimers is 6.9 ± 0.2 (mean ± standard error) nm. (b) Cartographic distribution of angular orientations of SP-A trimers on a spatial surface. Angular orientations of 2D averages of SP-A trimers shown in panel a were determined by IMAGIC-V. Inset shows the definitions for α and $\beta$ angles for a sphere with a unit length radius. Projected molecules in both foreground (squares) and background (plus) hemispheres are shown. Note that many of the 2D averages are represented near zero α and $\beta$ angles, i.e., clustered near the center of the cartogram.

*2D Organization of SP-A on Lipid Monolayers.* To determine the 3D structure of the SP-$A^{\Delta G8-P80}$ trimers and to identify their orientations on the lipid monolayers, images were grouped into 60 classes and averaged to yield 2D projections with an enhanced signal-to-noise ratio (Figure 2a). A trillium-like orientation of SP-A was predominant in the population of 2D averages. The average dimension of the particles in the 2D class averages (Figure 2a) was 6.9 ± 0.2 (mean ± standard error) nm, confirming the visual interpretation of the raw images as trimers (Figure 1c). Furthermore, when the angular orientations of these averages were mathematically determined, most of the molecules had small α and $\beta$ projection angles (Figure 2b). These data are consistent with the interpretation that the globular domains of SP-A interacted with lipid monolayers. This observation

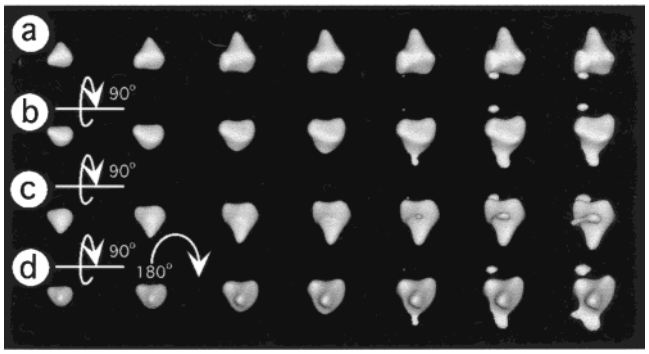


FIGURE 3: 3D structure of SP-A$^{\Delta G8-P80}$ trimers. (a−d) Four angular orientations (90° rotations) of the 3D image of the trimer (rows) at different surface contour threshold values (columns) are shown. Images in panel d are rotated 180° at the plane of the paper for easy visual interpretation (CRD at the top and neck at the bottom).

was also consistent with previous biochemical and mutagenisis-based experimental observations that implicated the interaction of the CRD with lipid membranes (*5*).

*3D Structure of SP-A Trimers.* Using these 2D class averages, the 3D structure of the SP-A$^{\Delta G8-P80}$ was reconstructed by IMAGIC-V (Figure 3). To determine the internal electron density levels and to identify the overall shape of the 3D structure of the molecule, the contour surface of the reconstructed image was examined at different density threshold levels by INSIGHT II/97 (Figure 3). The 3D image clearly showed the structure of SP-A trimers with identifiable CRDs and neck regions despite the limited range of orientations available and the consequent low resolution of the reconstruction. We interpreted these images to indicate that the CRD domains form the relatively flat face of the trimer (Figure 3a) that interacted with the lipid monolayer, whereas the neck region was considered to represent the relatively narrow domain pointing away from the lipid ligand surface (Figure 3b,d). The nonisotropic distribution of projection directions would ordinarily result in the reconstruction being stretched along the length of the neck/N-terminal end of the molecule. However, this feature was not strongly resolved in the reconstruction, probably because it was already poorly defined by negative stain. In the future, a higher resolution reconstruction could be obtained by the random conical tilting method (*35*). In the 2D projection averages (Figure 2a), it is already apparent that the globular domains are not arranged with precise 3-fold rotational symmetry. This asymmetry is also reflected in the 3D reconstitution and can be ascribed to the inherent flexibility of this macromolecule. This phenomenon has also been observed for SP-D trimers (*33*) and could contribute to ligand binding specificity.

*Molecular Organization of SP-A Monomer.* A homology-based molecular model for rat SP-A$^{\Delta G8-P80}$ was generated using INSIGHT II/97. Since the CRD of MBL is highly homologous to SP-A and the interchain disulfide bonds present in the CRD are conserved within the lectin family, these data were used to constrain the structure of the molecule. This approach provided most of the information necessary for assembly of the structural elements of SP-A. The energy minimized final model (Protein Data Bank I.D code 1DU8; Research Collaboratory for Structural Bioinformatics I.D code RCSB010373, Brookhaven, NY; http://www.rcsb.org/pdb) showed that the amino acid residues known to play a role in lipid interaction (*36*−*38*) were found

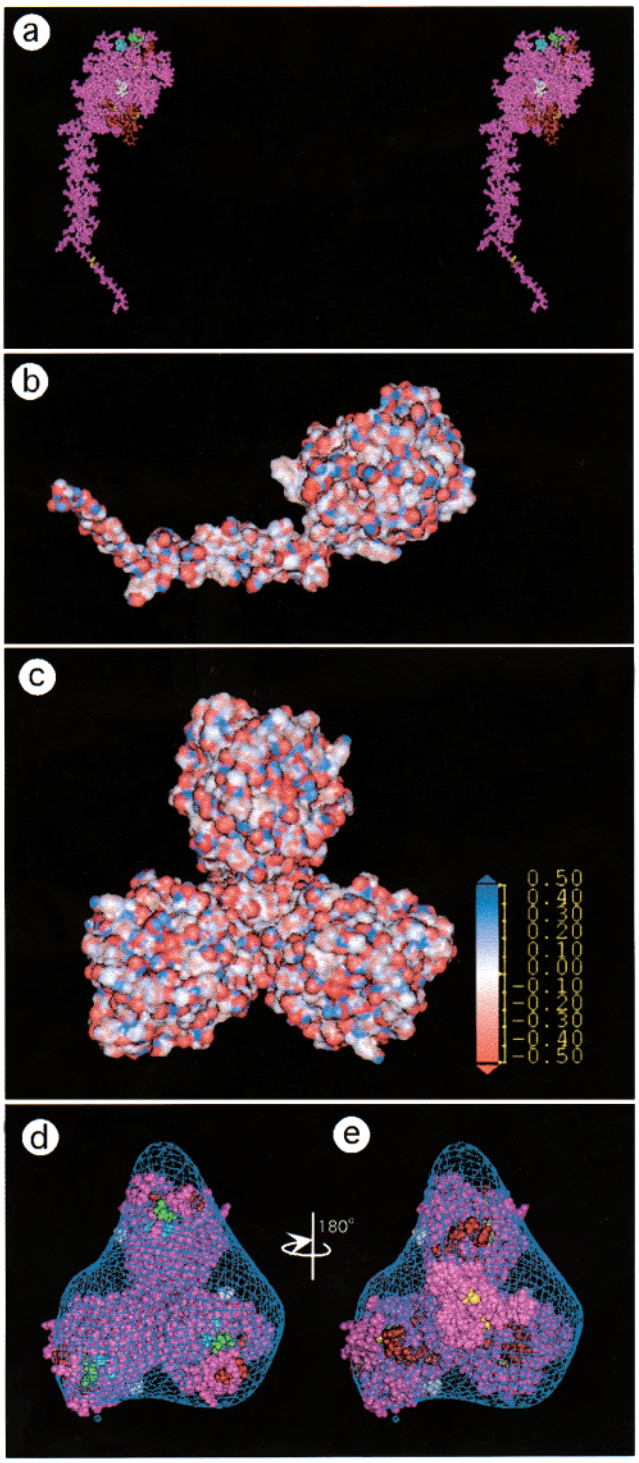


FIGURE 4: Molecular model of rat SP-A$^{\Delta G8-P80}$. (a) Stereoscopic view of the space filling model. Glu$^{195}$, blue; Arg$^{197}$, green; Cys, yellow; nonhomologous region to MBL, red. (b) Overall charge distribution of the SP-A$^{\Delta G8-P80}$ molecule is shown at side orientation with a Connolly surface. The color scheme is based on charge (negative, red; positive, blue). (c) Three identical rat SP-A$^{\Delta G8-P80}$ monomers are organized in such a way that the hydrophobic neck regions interact with each other. This trimer assembly is shown with a Connolly surface and has no charge clusters at the cleft. The trimer is fitted inside the electron density profile generated by single particle electron crystallography and 3D reconstruction. (d) View of the SP-A$^{\Delta G8-P80}$ at CRD−lipid monolayer interface and (e) after 180° rotation. Note that the CRDs of the trimers are asymmetrically organized.

near the surface of the globular domain (Figure 4a, blue and green). The solvent accessible Connolly surface of the

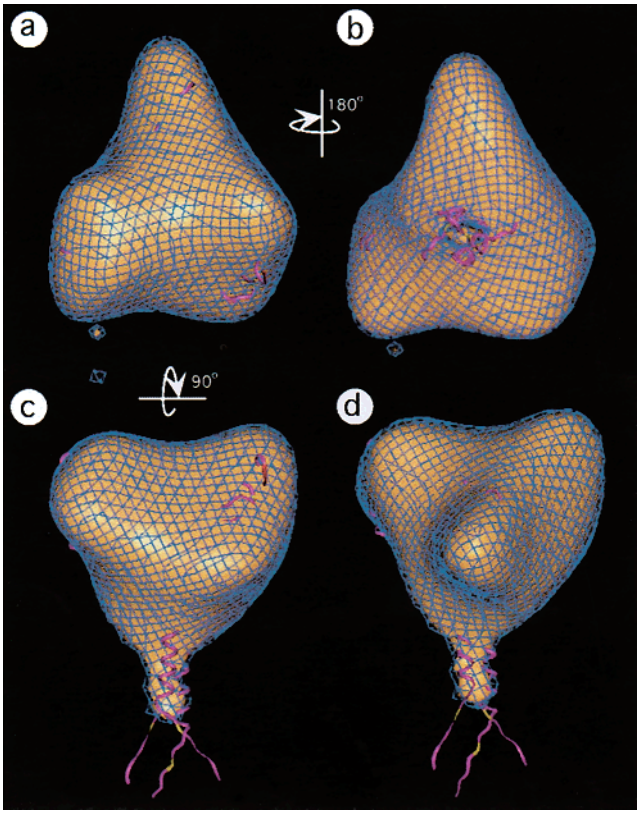


FIGURE 5: Organization of molecules within the electron density map. These images show the spatial organization of amino acid residues within the SP-A$^{\Delta G8-P80}$ trimer. Trimer molecular models in ribbon diagrams (purple) within the electron density shell (yellow solid surface with blue wire mesh contour) are shown. (a) CRD at lipid monolayer interface, (b)molecule after 180° rotation, and (c and d) side views of the molecules shown in panels a and b.

molecule, with its positively (blue) and negatively (red) charged residues, showed the overall molecular organization of the SP-A (Figure 4b,c). No apparent charge clusters were predicted for SP-A using this model.

*Molecular Organization of SP-A Trimers.* To determine further the relative locations of SP-A monomers in the 3D image of the SP-A trimer, three identical monomers were fitted into the electron density map (Figure 4c−e). The molecular models fit well within the electron density profile, and the amino acids that play a role in lipid binding (*36*−*40*) were found facing the lipid monolayer (Figure 4d). The amino acid residues 174−194, which may play a role in ligand binding specificity (*41*), were also located near the surface of the protein. A cleft was located in the middle of the three CRDs (Figures 4c,d and 6c−f), but the neck region was relatively distant from the lipid ligand (Figures 5 and 6). There were no stain penetrable pockets inside the molecule, suggesting that the globular domain was rather compact (Figures 3, 5, and 6). Some small loop regions protruded outside the electron density map (Figures 4−6) as would be expected from the limited resolution of the reconstruction. The images were consistent with a model in which the neck region holds the trimers together via protein−protein interaction but does not interact with the surface of the lipid monolayers.

The Asn$^{187}$ glycosylation site on the CRD was located at the side of each monomer significantly below the putative lipid−protein interface (Figure 4a). In the trimeric model,

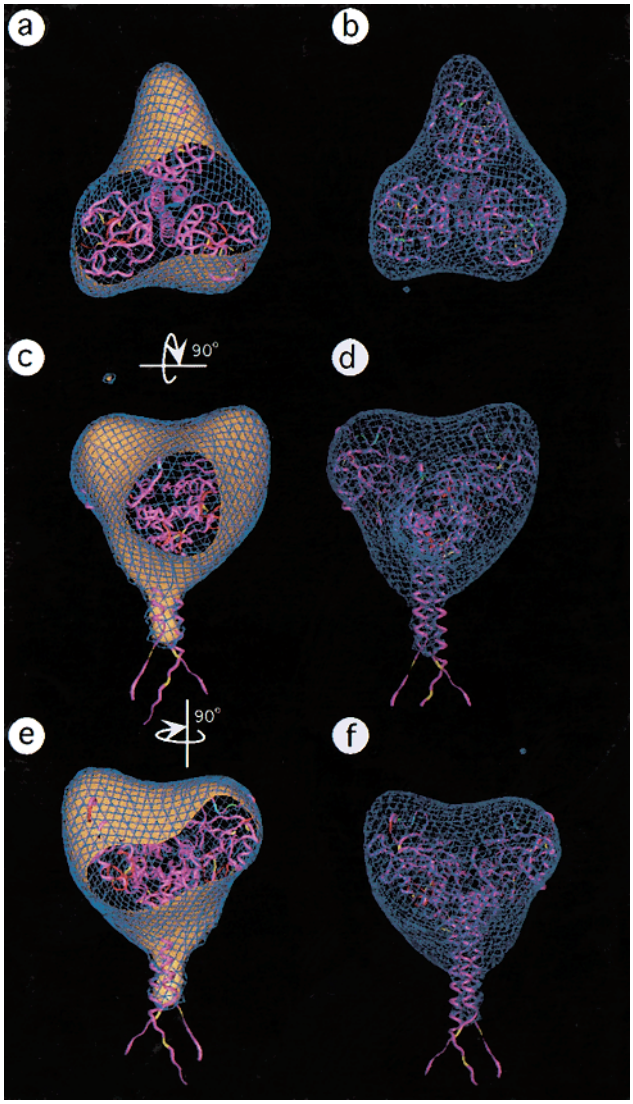


FIGURE 6: Molecular model organization inside the trimer. (a, c, and e) Electron density surface (solid) is cut open to show the internal organization of the molecular models, which are represented as ribbon diagrams. (b, d, and f) Molecular model is shown inside the wire mesh electron density contour surface. Color coding of the molecular model is the same as Figure 4.

Asn$^{187}$ of the monomers was located in such a way that the carbohydrate moieties would be predicted to occupy the electron-dense regions between the globular domains (Figure 4d,e). The MALDI-MS data indicated that the SP-A$^{\Delta G8-P80}$ molecule was modified by a carbohydrate moiety of approximately 1100 Da or 5−6 simple sugar residues (data not shown). Carbohydrate residues were not included in the model because of the uncertainty of the exact structure and composition of the oligosaccharide chains.

## DISCUSSION

Single particle electron crystallography allows the structural analysis of SP-A in association with a lipid monolayer. The exact nature of the CRD organization of SP-A has not been clearly established. We have shown here that a truncated form of SP-A, containing a deletion of the collagen-like domains, readily formed trimers (Figures 1 and 2). This result was in agreement with previous mutagenesis (*42*), biochemical, and chromatographic (*26*, *43*−*45*) observations. Dimen-

sions of the SP-A trimer determined from negatively stained images (~7 nm) were similar to those determined from the 2D averages (6.9 ± 0.2 nm). This value agreed well with the actual molecular distances between the periphery of each CRD (6.7, 7.2, and 6.4 nm; Figure 4) measured in this study. Low-resolution images of bovine SP-A trimers and their dimensions (6−8 nm) measured using negative staining and TEM have been reported by our group previously (*21, 23*). Similar dimensions (8 ± 2 nm) have also been reported for dog and human SP-As using platinum/palladium shadowed specimens (*20*). All of these values are within the range of the dimensions obtained in this study. Our present study has further provided information about the height of the CRD (8.4 nm). These data show that overall CRD trimers exist somewhat like a "thick funnel-shaped suction cup structure" (~2.2 and 7.0 nm internal and external diameters at the interface, respectively) with a dimpled cleft at the face (Figures 4−6).

SP-A is known to interact with lipid monolayers and bilayers (*22, 46, 47*), but the nature of these lipid−protein interactions has not been clearly established. Whether SP-A interacts with polar headgroups (*48*) or acyl chains (*49, 50*) of the lipid molecules is not clearly understood, but the interaction appears to be dependent on the physical and structural state of the lipids. Lipid monolayer studies suggest that SP-A interacts with polar headgroups of lipids (*48*). Furthermore, our previous TEM studies suggested that SP-A did not penetrate the lipid membranes to any significant extent (*21*). The present study showed that all three CRDs of SP-A$^{\Delta G8-P80}$ are oriented in a manner that could allow for simultaneous interaction with lipid monolayer. Molecular modeling indicated that the outer faces of the CRDs were most likely the regions of the interaction with lipids (Figure 4). Residues at the face of the CRD in our SP-A$^{\Delta G8-P80}$ model have previously been implicated in lipid interaction by targeted mutagenesis (*5*). These amino acid residues may directly interact with a lipid ligand or, alternatively, may contribute to local conformational changes required for lipid binding. By applying energy minimization algorithms to SP-A proteins with targeted modifications, it is possible to predict the effects of specific amino acid substitutions or posttranslational modifications on protein conformation using this molecular model.

The function(s) of the covalently linked carbohydrate moieties of the SP-As are not clearly understood. Our molecular model predicts that the glycosylation sites on the CRDs are located on the sides of each monomer between the globular domains and away from the putative protein−lipid interface (Figure 4d,e). As detailed above (*51, 52*), the lectin domain of SP-A is also located at the face of the CRD. Hence, it is unlikely that the carbohydrate moiety on any of the CRDs could interact with the lectin domain of another CRD within a single octadecamer assembly, but it is conceivable that such an interaction could occur between octadecamers.

Previous studies have suggested that the collagen-like domain of SP-A plays an important role in trimer formation. However, collagenase treatment of SP-A produces a fragment composed of only the neck and the CRD that forms trimers (*43, 44*). Similarly, chemical cross-linking studies indicate that SP-A$^{\Delta G8-P80}$ is trimeric (*42*). On the basis of structural data obtained with MBL (*30, 32*) and SP-D (*33, 53*), these results suggest that the neck region is sufficient for trimerization. Our images and molecular model confirm that SP-A$^{\Delta G8-P80}$ is trimeric and that the CRDs of SP-A are spatially separated but held together by interactions within the neck region. Our results also show that the neck regions of SP-A do not appear to interact with the lipid ligand (Figures 4−6). Although secondary structure predictions based on the primary structure of the molecule suggest the existence of an amphipathic α-helix in the neck regions (*17*) and short synthetic peptides using such sequences (*18, 45*) may interact with lipid membranes, the neck region of SP-A appears to be primarily involved in intersubunit interactions.

In summary, trimeric fragments of SP-A composed primarily of the C-terminal half of the molecule were imaged by TEM in association with a lipid monolayer. We found that the CRDs of SP-A form a trillium structure that is anchored by the neck domain. The CRDs are asymmetrically distributed about the center point, in a manner that is similar to what has been reported for another member of the collectin family, SP-D. We developed a trimeric homology-based molecular model for SP-A using the primary structure of SP-A and the X-ray crystallographic coordinates of MBL, by making assumptions about the conformation of conserved domains and by energy minimization. The model was fitted into the electron density map created by single particle electron crystallography and computational 3D reconstruction. We found that the CRD of SP-A had a relatively flat face that interacted with the lipid monolayer. Amino acids that have previously been implicated in phospholipid interactions mapped to the protein−phospholipid interface of the model. There were no charge clusters as had been reported for SP-D. The carbohydrate moiety was predicted to occupy the space between CRDs, in a location that would not sterically interfere with ligand binding.

## ACKNOWLEDGMENT

We thank Mamatha Damodarasamy for technical support, George Smulian for MALDI-MS analysis, and Wen Li for helpful discussions regarding the angular reconstitution program.

## REFERENCES

1. King, R. J., Klass, D. J., Gikas, E. G., and Clements, J. A. (1973) *Am. J. Physiol. 224*, 788−95.
2. Wright, J. R. (1997) *Physiol. Rev. 77*, 931−62.
3. Eggleton, P., and Reid, K. B. (1999) *Curr. Opin. Immunol. 11*, 28−33.
4. Wright, J. R., Borchelt, J. D., and Hawgood, S. (1989) *Proc. Natl. Acad. Sci. U.S.A. 86*, 5410−4.
5. McCormack, F. X. (1998) *Biochim. Biophys. Acta 1408*, 109−31.
6. Korfhagen, T. R., Bruno, M. D., Ross, G. F., Huelsman, K. M., Ikegami, M., Jobe, A. H., Wert, S. E., Stripp, B. R., Morris, R. E., Glasser, S. W., Bachurski, C. J., Iwamoto, H. S., and Whitsett, J. A. (1996) *Proc. Natl. Acad. Sci. U.S.A. 93*, 9594−9.
7. Ikegami, M., Korfhagen, T. R., Whitsett, J. A., Bruno, M. D., Wert, S. E., Wada, K., and Jobe, A. H. (1998) *Am. J. Physiol. 275*, L247−54.
8. Elhalwagi, B. M., Zhang, M., Ikegami, M., Iwamoto, H. S., Morris, R. E., Miller, M. L., Dienger, K., and McCormack, F. X. (1999) *Am. J. Respir. Cell Mol. Biol. 21*, 380−7.
9. LeVine, A. M., Gwozdz, J., Stark, J., Bruno, M., Whitsett, J., and Korfhagen, T. (1999) *J. Clin. Invest. 103*, 1015−21.

10. Hickman-Davis, J., Gibbs-Erwin, J., Lindsey, J. R., and Matalon, S. (1999) *Proc. Natl. Acad. Sci. U.S.A. 96*, 4953−8.
11. Ikegami, M., Korfhagen, T. R., Bruno, M. D., Whitsett, J. A., and Jobe, A. H. (1997) *Am. J. Physiol. 272*, L479−85.
12. Botas, C., Poulain, F., Akiyama, J., Brown, C., Allen, L., Goerke, J., Clements, J., Carlson, E., Gillespie, A. M., Epstein, C., and Hawgood, S. (1998) *Proc. Natl. Acad. Sci. U.S.A. 95*, 11869−74.
13. Poulain, F. R., Akiyama, J., Allen, L., Brown, C., Chang, R., Goerke, J., Dobbs, L., and Hawgood, S. (1999) *Am. J. Respir. Cell Mol. Biol. 20*, 1049−58.
14. Korfhagen, T. R., Sheftelyevich, V., Burhans, M. S., Bruno, M. D., Ross, G. F., Wert, S. E., Stahlman, M. T., Jobe, A. H., Ikegami, M., Whitsett, J. A., and Fisher, J. H. (1998) *J. Biol. Chem. 273*, 28438−43.
15. Benson, B., Hawgood, S., Schilling, J., Clements, J., Damm, D., Cordell, B., and White, R. T. (1985) *Proc. Natl. Acad. Sci. U.S.A. 82*, 6379−83.
16. Sano, K., Fisher, J., Mason, R. J., Kuroki, Y., Schilling, J., Benson, B., and Voelker, D. (1987) *Biochem. Biophys. Res. Commun. 144*, 367−74.
17. McLean, L. R., Lewis, J. E., Hagaman, K. A., Owen, T. J., and Jackson, R. L. (1993) *Biochim. Biophys. Acta 1166*, 31−8.
18. Walther, F. J., David-Cu, R., Leung, C., Bruni, R., Hernandez-Juviel, J., Gordon, L. M., and Waring, A. J. (1996) *Pediatr. Res. 39*, 938−46.
19. King, R. J., Simon, D., and Horowitz, P. M. (1989) *Biochim. Biophys. Acta 1001*, 294−301.
20. Voss, T., Eistetter, H., Schafer, K. P., and Engel, J. (1988) *J. Mol. Biol. 201*, 219−27.
21. Palaniyar, N., Ridsdale, R. A., Holterman, C. E., Inchley, K., Possmayer, F., and Harauz, G. (1998) *J. Struct. Biol. 122*, 297−310.
22. Palaniyar, N., Ridsdale, R. A., Possmayer, F., and Harauz, G. (1998) *Biochem. Biophys. Res. Commun. 250*, 131−6.
23. Ridsdale, R. A., Palaniyar, N., Holterman, C. E., Inchley, K., Possmayer, F., and Harauz, G. (1999) *Biochim. Biophys. Acta 1453*, 23−34.
24. Palaniyar, N., Ridsdale, R. A., Hearn, S. A., Heng, Y. M., Ottensmeyer, F. P., Possmayer, F., and Harauz, G. (1999) *Am. J. Physiol. 276*, L631−41.
25. Palaniyar, N., Ridsdale, R. A., Hearn, S. A., Possmayer, F., and Harauz, G. (1999) *Am. J. Physiol. 276*, L642−9.
26. McCormack, F. X., Pattanajitvilai, S., Stewart, J., Possmayer, F., Inchley, K., and Voelker, D. R. (1997) *J. Biol. Chem. 272*, 27971−9.
27. Beniac, D. R., Luckevich, M. D., Czarnota, G. J., Tompkins, T. A., Ridsdale, R. A., Ottensmeyer, F. P., Moscarello, M. A., and Harauz, G. (1997) *J. Biol. Chem. 272*, 4261−8.
28. Beniac, D. R., Wood, D. D., Palaniyar, N., Ottensmeyer, F. P., Moscarello, M. A., and Harauz, G. (1999) *Mol. Cell. Biol. Res. Commun. 1*, 48−51.
29. van Heel, M., Harauz, G., Orlova, E. V., Schmidt, R., and Schatz, M. (1996) *J. Struct. Biol. 116*, 17−24.
30. Sheriff, S., Chang, C. Y., and Ezekowitz, R. A. (1994) *Nat. Struct. Biol. 1* 789−94.
31. Weis, W. I., Taylor, M. E., and Drickamer, K. (1998) *Immunol. Rev. 163*, 19−34.
32. Weis, W. I., and Drickamer, K. (1994) *Structure 2*, 1227−40.
33. Hakansson, K., Lim, N. K., Hoppe, H. J., and Reid, K. B. (1999) *Structure Fold Des. 7*, 255−64.
34. Muller, S. A., and Engel, A. (1998) *J. Struct. Biol. 121*, 219−30.
35. Radermacher, M. (1998) *J. Electron. Microsc. Tech. 9*, 359−394.
36. McCormack, F. X., Kuroki, Y., Stewart, J. J., Mason, R. J., and Voelker, D. R. (1994) *J. Biol. Chem. 269*, 29801−7.
37. Tsunezawa, W., Sano, H., Sohma, H., McCormack, F. X., Voelker, D. R., and Kuroki, Y. (1998) *Biochim. Biophys. Acta 1387*, 433−46.
38. Sano, H., Kuroki, Y., Honma, T., Ogasawara, Y., Sohma, H., Voelker, D. R., and Akino, T. (1998) *J. Biol. Chem. 273*, 4783−9.
39. McCormack, F. X., Stewart, J., Voelker, D. R., and Damodarasamy, M. (1997) *Biochemistry 36*, 13963−71.
40. Pattanajitvilai, S., Kuroki, Y., Tsunezawa, W., McCormack, F. X., and Voelker, D. R. (1998) *J. Biol. Chem. 273*, 5702−7.
41. Chiba, H., Sano, H., Saitoh, M., Sohma, H., Voelker, D. R., Akino, T., and Kuroki, Y. (1999) *Biochemistry 38*, 7321−31.
42. McCormack, F. X., Damodarasamy, M., and Elhalwagi, B. M. (1999) *J. Biol. Chem. 274*, 3173−81.
43. Haagsman, H. P., White, R. T., Schilling, J., Lau, K., Benson, B. J., Golden, J., Hawgood, S., and Clements, J. A. (1989) *Am. J. Physiol. 257*, L421−9.
44. Haagsman, H. P., Sargeant, T., Hauschka, P. V., Benson, B. J., and Hawgood, S. (1990) *Biochemistry 29*, 8894−900.
45. Ross, G. F., Notter, R. H., Meuth, J., and Whitsett, J. A. (1986) *J. Biol. Chem. 261*, 14283−91.
46. Ruano, M. L., Nag, K., Worthman, L. A., Casals, C., Perez-Gil, J., and Keough, K. M. (1998) *Biophys. J. 74*, 1101−9.
47. Yu, S. H., McCormack, F. X., Voelker, D. R., and Possmayer, F. (1999) *J. Lipid Res. 40*, 920−9.
48. Yu, S. H., and Possmayer, F. (1998) *J. Lipid Res. 39*, 555−68.
49. King, R. J., Carmichael, M. C., and Horowitz, P. M. (1983) *J. Biol. Chem. 258*, 10672−80.
50. Kuroki, Y., and Akino, T. (1991) *J. Biol. Chem. 266*, 3068−73.
51. Weis, W. I., Drickamer, K., and Hendrickson, W. A. (1992) *Nature 360*, 127−34.
52. Drickamer, K. (1992) *Nature 360*, 183−6.
53. Hoppe, H. J., Barlow, P. N., and Reid, K. B. (1994) *FEBS Lett. 344*, 191−5.

BI992793B